

On Probing θ_{23} in Neutrino Telescopes

Sandhya Choubey^{a*}, Viviana Niro^{b†}, Werner Rodejohann^{b‡}

^a*Harish-Chandra Research Institute,
Chhatnag Road, Jhansi, 211019 Allahabad, India*

^b*Max-Planck-Institut für Kernphysik,
Postfach 103980, D-69029 Heidelberg, Germany*

Abstract

Among all neutrino mixing parameters, the atmospheric neutrino mixing angle θ_{23} introduces the strongest variation on the flux ratios of ultra high energy neutrinos. We investigate the potential of these flux ratio measurements at neutrino telescopes to constrain θ_{23} . We consider astrophysical neutrinos originating from pion, muon-damped and neutron sources and make a comparative study of their sensitivity reach to θ_{23} . It is found that neutron sources are most favorable for testing deviations from maximal θ_{23} . Using a χ^2 analysis, we show in particular the power of combining (i) different flux ratios from the same type of source, and also (ii) combining flux ratios from different astrophysical sources. We include in our analysis “impure” sources, i.e., deviations from the usually assumed initial (1 : 2 : 0), (0 : 1 : 0) or (1 : 0 : 0) flux compositions.

*email: sandhya@hri.res.in

†email: viviana.niro@mpi-hd.mpg.de

‡email: werner.rodejohann@mpi-hd.mpg.de

1 Introduction

Dedicated facilities spanning km^2 of area for detecting ultra high energy neutrino coming from astrophysical sources are under construction (IceCube [1, 2]) or consideration (KM3Net [3]). Motivated by this, a significant number of papers has been devoted in recent years to the phenomenon of neutrino mixing of high-energy astrophysical neutrinos [4–22]. That neutrinos are massive and therefore mix has been proved beyond any doubt by observations of neutrinos coming from the Sun [23], atmosphere [24], reactors [25] and accelerators [26, 27]. The most recent limits on the mass-squared differences and the mixing angles can be found in [28]. The mass splitting associated with solar neutrino oscillations is $\Delta m_{21}^2 \simeq 7.6 \times 10^{-5} \text{ eV}^2$, while that associated with atmospheric neutrinos is $|\Delta m_{31}^2| \simeq 2.5 \times 10^{-3} \text{ eV}^2$. Because the oscillation lengths corresponding to these mass-squared differences are much smaller than astrophysical distances, the oscillations get averaged out for the astrophysical neutrinos. However, the non-trivial flavor mixing in the lepton sector still modifies the neutrinos fluxes on their way from the source to the detector. This opens up the possibility to obtain information on the mixing angles and the CP phase of the PMNS matrix. This information would be complementary to the already impressive existing and expected data from current and future experiments devoted purely to neutrino oscillations.

Ultra high energy (UHE) neutrinos are expected to come from decay of pions, muons and/or neutrons. Therefore, even though the absolute numbers of UHE neutrinos are uncertain by a huge amount, the relative proportions of the initial flux compositions $\Phi_e^0 : \Phi_\mu^0 : \Phi_\tau^0$ are known. Here Φ_α^0 with $\alpha = e, \mu, \tau$ is the initial flux of a neutrino with flavor α . This ratio is $(1 : 2 : 0)$, $(0 : 1 : 0)$ and $(1 : 0 : 0)$ for pion, muon-damped and neutron sources, respectively. Hence, working with the flux ratios of different flavors is considered to be much less model dependent than working with absolute fluxes. One complication which still arises is that in general one expects corrections [8, 19, 30] to the usually assumed “pure” initial flux compositions. For instance, instead of $(\Phi_e^0 : \Phi_\mu^0 : \Phi_\tau^0) = (1 : 2 : 0)$, one might initially have $(1 : 2(1 - \zeta) : 0)$, with ζ being around $= 0.1$ [30]. Not taking such deviations into account can lead to wrong conclusions about the neutrino parameters [22].

Currently the mixing angle θ_{23} is one of the least known besides θ_{13} , the CP phase and the neutrino mass hierarchy. In fact, the quantity $\sin^2 \theta_{23}$ is uncertain by about $\pm 33\%$ at 3σ . Information on this mixing angle and its deviation from maximality can be tested in future atmospheric neutrino experiments [31, 32]. Using the zenith angle dependence of the muon events in atmospheric neutrino data, one would be able to restrict $\sin^2 \theta_{23}$ to within $\pm 24\%$ with 1.84 MTy (megaton-year) data in water Cerenkov detectors and to within $\pm 30\%$ with 250 kTy data in large magnetized iron calorimeters [33]. Atmospheric neutrino data could also be used very effectively to give us the “octant” (whether $\theta_{23} < \pi/4$ or $> \pi/4$) of θ_{23} , if indeed θ_{23} turns out to be non-maximal. The sub-GeV electron events in water Cerenkov detectors carry information on the θ_{23} octant through the Δm_{21}^2 -driven sub-dominant oscillations [31]. The multi-GeV muon events in large magnetized iron calorimeters have sensitivity to Earth matter effects which in turn depend on θ_{23} and its octant [32]. Long baseline experiments would also give very good sensitivity to $\sin^2 \theta_{23}$:

the combined 5 year data from MINOS, ICARUS, OPERA, T2K and NO ν A is expected to constrain $\sin^2 \theta_{23}$ to within $\pm 20\%$ around its maximal value [34].

In this letter we will focus on the possibility to constrain the atmospheric neutrino mixing angle θ_{23} from measurements of flux ratios at neutrino telescopes. After arguing that their dependence on this angle is strongest among the neutrino mixing parameters, we discuss its possible constraints using a χ^2 analysis. We quantify that combining different sources leads to stronger constraints on θ_{23} . If different flux ratios from different neutrino sources are combined (those are pion, muon-damped and neutron sources), even better constraints are possible. Neutron beam sources turn out to be the most interesting ones. We include the possibility of “impure sources” in our analysis and investigate their impact for the first time in a statistical analysis.

We begin by discussing the flux ratios of UHE at the neutrino telescopes in Section 2. In Section 3 we introduce our χ^2 function and use it to give prospective bounds on θ_{23} using the flux ratios. We end in Section 4 with a summary of our results and conclusions.

2 Neutrino Mixing and Neutrino Telescopes

Astrophysical sources will generate fluxes of electron, muon and tau neutrinos, denoted by Φ_e^0 , Φ_μ^0 and Φ_τ^0 , respectively. As a consequence of non-trivial neutrino mixing, it is not this initial flux composition which arrives at terrestrial detectors. In fact, what is measurable is given by

$$\begin{pmatrix} \Phi_e \\ \Phi_\mu \\ \Phi_\tau \end{pmatrix} = \begin{pmatrix} P_{ee} & P_{e\mu} & P_{e\tau} \\ P_{\mu e} & P_{\mu\mu} & P_{\mu\tau} \\ P_{\tau e} & P_{\tau\mu} & P_{\tau\tau} \end{pmatrix} \begin{pmatrix} \Phi_e^0 \\ \Phi_\mu^0 \\ \Phi_\tau^0 \end{pmatrix}, \quad (1)$$

where the neutrino mixing probability is

$$P_{\alpha\beta} = P_{\beta\alpha} = \sum_i |U_{\alpha i}|^2 |U_{\beta i}|^2 \quad (2)$$

and U is the lepton mixing matrix. The flavor mixing matrix P comprises of the individual $P_{\alpha\beta}$ elements. The current best-fit values as well as the allowed 1σ and 3σ ranges of the oscillation parameters are [28]:

$$\begin{aligned} \sin^2 \theta_{12} &= 0.32_{-0.02, 0.06}^{+0.02, 0.08}, \\ \sin^2 \theta_{23} &= 0.45_{-0.06, 0.13}^{+0.09, 0.19}, \\ \sin^2 \theta_{13} &< 0.019 (0.050). \end{aligned} \quad (3)$$

These mixing angles can be related to elements of the PMNS mixing matrix via

$$U = \begin{pmatrix} c_{12} c_{13} & s_{12} c_{13} & s_{13} e^{-i\delta} \\ -s_{12} c_{23} - c_{12} s_{23} s_{13} e^{i\delta} & c_{12} c_{23} - s_{12} s_{23} s_{13} e^{i\delta} & s_{23} c_{13} \\ s_{12} s_{23} - c_{12} c_{23} s_{13} e^{i\delta} & -c_{12} s_{23} - s_{12} c_{23} s_{13} e^{i\delta} & c_{23} c_{13} \end{pmatrix}, \quad (4)$$

where $c_{ij} = \cos \theta_{ij}$, $s_{ij} = \sin \theta_{ij}$. The CP phase δ is unknown. Because the mass-squared differences drop out of the mixing probabilities, and solar neutrino mixing is neither maximal, zero nor $\pi/2$, no transition probability $P_{\alpha\beta}$ with $\alpha \neq \beta$ is zero and no survival probability $P_{\alpha\alpha}$ is one. Consequently, high energy astrophysical neutrinos will always mix. To be precise, at 1σ and 3σ the entries of the flavor conversion matrix $P_{\alpha\beta}$ are

$$P = \begin{cases} \begin{pmatrix} 0.53 \div 0.58 & 0.18 \div 0.30 & 0.16 \div 0.27 \\ \cdot & 0.34 \div 0.44 & 0.35 \div 0.40 \\ \cdot & \cdot & 0.35 \div 0.47 \end{pmatrix} & (\text{at } 1\sigma), \\ \begin{pmatrix} 0.47 \div 0.62 & 0.12 \div 0.35 & 0.11 \div 0.34 \\ \cdot & 0.33 \div 0.51 & 0.30 \div 0.40 \\ \cdot & \cdot & 0.33 \div 0.53 \end{pmatrix} & (\text{at } 3\sigma). \end{cases} \quad (5)$$

As is obvious from Eq. (3), a good zeroth order description of neutrino mixing is tribimaximal mixing [35],

$$U \simeq U_{\text{TBM}} = \begin{pmatrix} \sqrt{\frac{2}{3}} & \frac{1}{\sqrt{3}} & 0 \\ -\frac{1}{\sqrt{6}} & \frac{1}{\sqrt{3}} & -\frac{1}{\sqrt{2}} \\ -\frac{1}{\sqrt{6}} & \frac{1}{\sqrt{3}} & \frac{1}{\sqrt{2}} \end{pmatrix}. \quad (6)$$

Therefore, it proves in particular useful to expand in terms of¹

$$|U_{e3}| \text{ and } \epsilon \equiv \frac{\pi}{4} - \theta_{23} = \frac{1}{2} - \sin^2 \theta_{23} + \mathcal{O}(\epsilon^3). \quad (7)$$

For simplicity, we fix from now on for analytical considerations $\sin^2 \theta_{12}$ to $\frac{1}{3}$. This is a valid approximation for obtaining simple analytical expressions, but we stress that the numerical results to be presented in this paper are obtained with the exact expressions. The result for the flavor mixing matrix is

$$P \simeq \begin{pmatrix} \frac{5}{9} & \frac{2}{9} & \frac{2}{9} \\ \cdot & \frac{7}{18} & \frac{7}{18} \\ \cdot & \cdot & \frac{7}{18} \end{pmatrix} + \Delta \begin{pmatrix} 0 & 1 & -1 \\ \cdot & -1 & 0 \\ \cdot & \cdot & 1 \end{pmatrix} + \frac{1}{2} \overline{\Delta}^2 \begin{pmatrix} 0 & 0 & 0 \\ \cdot & 1 & -1 \\ \cdot & \cdot & 1 \end{pmatrix}, \quad (8)$$

where the universal first [12, 15] and second [21, 22] order correction terms are

$$\begin{aligned} \Delta &= \frac{1}{9} \left(\sqrt{2} \cos \delta |U_{e3}| + 4\epsilon \right), \\ \overline{\Delta}^2 &= \frac{4}{9} \left(2 \cos^2 \delta |U_{e3}|^2 + 7\epsilon^2 - \sqrt{2} \cos \delta |U_{e3}| \epsilon \right). \end{aligned} \quad (9)$$

We have omitted here small and usually negligible terms in the expansion which only contain $|U_{e3}|^2$, see Refs. [21, 22]. Note that $\overline{\Delta}^2$ can be written as $\frac{1}{9} (2\sqrt{2} \cos \delta |U_{e3}| - \epsilon)^2 + 3\epsilon^2$

¹An expansion up to second order around zero $|U_{e3}|$, maximal θ_{23} and $\sin^2 \theta_{12} = \frac{1}{3}$ can be found in Refs. [21, 22].

and therefore is positive semi-definite. In addition, $\overline{\Delta}^2$ turns out to be often larger than the first order term Δ [21, 22]. To be quantitative,

$$\begin{aligned} \text{at } 1\sigma : & \quad -0.043 \leq \Delta \leq 0.069 \quad , \quad \overline{\Delta}^2 \leq 0.061 \quad , \\ \text{at } 3\sigma : & \quad -0.104 \leq \Delta \leq 0.117 \quad , \quad \overline{\Delta}^2 \leq 0.179 \quad . \end{aligned} \quad (10)$$

The dependence of Δ and $\overline{\Delta}^2$ on θ_{12} is very weak [21, 22]. From the expressions for Δ and $\overline{\Delta}^2$ it is clear that their dependence on the atmospheric neutrino mixing angle θ_{23} is stronger than on $\cos \delta |U_{e3}|$. It is the large prefactor in front of ϵ and ϵ^2 which is the reason for this behavior. In addition, these prefactors are larger than the ones related to $|U_{e3}|$. Hence, the dependence on $|U_{e3}|$ is weaker and smeared by the additional dependence on $\cos \delta$. This is why we are interested here in effects of deviations from maximal atmospheric neutrino mixing.

The neutrino sources we assume are pion, muon-damped [36] and neutron [37] sources, with initial flux compositions of

$$(\Phi_e^0 : \Phi_\mu^0 : \Phi_\tau^0) = \begin{cases} (1 : 2(1 - \zeta) : 0) & \text{pion ,} \\ (\eta : 1 : 0) & \text{muon-damped ,} \\ (1 : \eta : 0) & \text{neutron .} \end{cases} \quad (11)$$

By introducing small $\zeta, \eta \ll 1$ [22], we have allowed here for impurities in the initial compositions, which can be expected on general grounds [8, 19, 30].

Turning to the observable flavor ratios [38, 39], the most frequently considered is the ratio of muon neutrinos to all other flavors:

$$T = \frac{\Phi_\mu}{\Phi_e + \Phi_\mu + \Phi_\tau} = \frac{\Phi_\mu}{\Phi_{\text{tot}}} . \quad (12)$$

Using again $\sin^2 \theta_{12} = \frac{1}{3}$ and expanding in terms of the small parameters $|U_{e3}|$, $\epsilon = \frac{\pi}{4} - \theta_{23}$ as well as ζ or η one finds [22]

$$T \simeq \begin{cases} \frac{1}{3} \left(1 - \Delta + \overline{\Delta}^2 - \frac{1}{9} \zeta \right) , & \text{pion } (1 : 2(1 - \zeta) : 0) , \\ \frac{7}{18} - \Delta + \frac{1}{2} \overline{\Delta}^2 - \frac{1}{6} \eta , & \text{muon-damped } (\eta : 1 : 0) , \\ \frac{2}{9} + \Delta + \frac{1}{6} \eta , & \text{neutron beam } (1 : \eta : 0) . \end{cases} \quad (13)$$

The second order correction $\overline{\Delta}^2$ appears only in $P_{\mu\mu}$, $P_{\mu\tau}$ and $P_{\tau\tau}$, and therefore does not affect T for neutron sources. Hence, the dependence on $\sin^2 \theta_{23}$ can be described to an excellent approximation as quadratic for pion and muon-damped sources, but linear for neutron sources. We show in the left panel of Fig. 1 the ratio T as a function of $\sin^2 \theta_{23}$ and $\sin \theta_{13}$ for the three pure sources (i.e., $\zeta = \eta = 0$). Plots are shown for fixed $\sin^2 \theta_{12} = 0.32$ and three values of δ . The stronger dependence on $\sin^2 \theta_{23}$ is clearly seen. Fig. 2 focusses on

the dependence of the flux ratios on $\sin^2 \theta_{23}$. We have taken the range $\sin^2 \theta_{12} = 0.32 \pm 0.02$, $\sin^2 \theta_{13} < 0.005$ and $0 \leq \delta < 2\pi$. We have also marked the current 1σ and 3σ allowed ranges of $\sin^2 \theta_{23}$ for comparison. We reiterate that these plots are for $\zeta = \eta = 0$. Note that because of larger prefactors in front of ζ and η in Eq. (13), impurities are expected to have stronger impact for muon-damped and neutron sources. Finally, we stress that the correction factors Δ and $\overline{\Delta}^2$, which can both be $\mathcal{O}(0.1)$, are added to a number around 1 for pion sources, but to a number around 0.4 for muon-damped and 0.2 for neutron sources. Hence, neutron sources are expected to be the most useful to constrain θ_{23} .

Another ratio which can be considered is the ratio of electron to tau neutrinos,

$$R = \frac{\Phi_e}{\Phi_\tau} . \quad (14)$$

For the three neutrino sources one finds [22]

$$R = \frac{\Phi_e}{\Phi_\tau} \simeq \begin{cases} 1 + 3\Delta(1 + \Delta) + \overline{\Delta}^2 + \frac{1}{3}\zeta, & \text{pion } (1 : 2(1 - \zeta) : 0) , \\ \frac{4}{7} \left(1 + \frac{9}{2}\Delta + \frac{9}{7}\overline{\Delta}^2 + \frac{27}{14}\eta \right) , & \text{muon-damped } (\eta : 1 : 0) , \\ \frac{5}{2} \left(1 + \frac{9}{2}\Delta - \frac{27}{20}\eta \right) , & \text{neutron beam } (1 : \eta : 0) . \end{cases} \quad (15)$$

Comparing these expressions with the ones for T in Eq. (13), we note that in case of pion and muon-damped sources the first and second order correction terms Δ and $\overline{\Delta}^2$ are added in R , whereas they are subtracted in T . Recalling that ϵ and ϵ^2 appear with equal sign in Δ and $\overline{\Delta}^2$, we expect stronger dependence on θ_{23} in R than in T . This is illustrated in the right panels of Figs. 1 and 2, where we display R as a function of $\sin \theta_{13}$ and $\sin^2 \theta_{23}$. Again, the dependence on $\sin^2 \theta_{23}$ is basically quadratic for pion and muon-damped sources, whereas it is linear for neutron beams. The effect of impurity will be in general larger for R , because of the larger prefactors in front of ζ and η . Note also that the parameters ζ and η appear in R with opposite sign compared to T .

3 Statistical Analysis

To statistically investigate the prospects of constraining θ_{23} with neutrino telescopes, we turn to a χ^2 analysis. First we discuss the case in which only T is measured. Let us define the χ^2 function to be minimized as:

$$\chi^2 = \left(\frac{T_{\text{th}} - T_{\text{exp}}}{\sigma_{T_{\text{exp}}}} \right)^2 + \sum_{ij=12,13} \left(\frac{s_{ij}^2 - (s_{ij}^2)_{\text{best-fit}}}{\sigma_{s_{ij}^2}} \right)^2 , \quad (16)$$

where T_{th} and T_{exp} are the theoretically predicted and experimentally measured T ratios, respectively, and $\sigma_{T_{\text{exp}}}$ is the 1σ uncertainty of the measured value T_{exp} in the neutrino telescope.

We take into account the possible uncertainty of the initial flux composition by constructing different χ^2 functions for different initial flavor compositions and then define the allowed region of $\sin^2 \theta_{23}$ as the maximum range obtained by combining the different functions. The errors on T for the different sources are expected to lie in the range 15-25% after a decade of running of the experiment. It is expected that the error on pion sources will be less than those on muon-damped and neutron sources. Therefore, we present most of our results for fixed assumed errors on the flux ratio T as 10% for pion, 20% for muon-damped and 15% for neutron sources. In what regards R , the assumed errors are 15% for pion, 25% for muon-damped and 20% for neutron sources. In general one expects larger errors for R than on T : muon neutrinos can be identified at neutrino telescopes for energies greater than 100 GeV through characteristic muon tracks. Electron and tau neutrinos, can be identified through showers and effects like “double bang” events, respectively, only for higher energies, above 10^6 GeV. Recall that muon-damping is expected to happen in a generic pion source for a particular and limited energy range, in which the muon is absorbed before decaying [36]. Hence, less statistics for muon-damped sources with respect to pion sources is expected. Concerning neutron sources, we have chosen an error greater than the one for pion sources, because they are expected to be characterized in an energy range covered by atmospheric neutrino background [37]. Therefore the systematic error in this case might be greater than the one for pion sources. Hence, we have chosen a hierarchy among the errors for the different types of sources. However, the values for the errors taken above are just one choice for the errors, which could be different from what has been chosen above. To take into this fact and to show the impact of the errors on our analysis, we will also show the results as a function of the error on T .

We generate the prospective data T_{exp} for two sets of mixing angles which we assume as “true” and minimize the χ^2 function to obtain bounds on the measured θ_{23} at neutrino telescopes. In the fit we allow θ_{12} , θ_{13} and δ to take any value in their physically allowed ranges. The second term in Eq. (16) takes into account the “priors” on the mixing angles θ_{12} and θ_{13} , on which we expect better constraints by the time we get the data on UHE neutrinos at neutrino telescopes. For the 1σ uncertainty on θ_{12} we use the range given in Eq. (3), while for θ_{13} we use the following upper bound:

$$\sin^2 2\theta_{13} < 0.03 \text{ at } 90\% \text{ C.L.} , \quad (17)$$

which corresponds to the absence of a signal in the Double CHOOZ experiment after three years of operation with both detectors [40]. We have considered in our analysis this specific case and we have studied the consequences that can be inferred on the atmospheric mixing angle. This situation has been considered as an optimistic scenario. Indeed, larger values of θ_{13} than the ones we have chosen would worsen the sensitivity on θ_{23} .

We generate T_{exp} and show results for two sets of true values for the mixing parameters:

1. $\sin^2 \theta_{12} = 1/3$, $\sin^2 \theta_{13} = 0$ and $\sin^2 \theta_{23} = 1/2$ (Scenario TBM) ,
2. $\sin^2 \theta_{12} = 0.32$, $\sin^2 \theta_{13} = 0$ and $\sin^2 \theta_{23} = 0.6$ (Scenario 2) .

Scenario TBM gives T_{exp} (and R_{exp}) corresponding to their “tri-bimaximal values”, i.e., the zeroth order terms from Eqs. (13) and (15). Scenario 2 gives $T_{\text{exp}} = 0.36, 0.45,$ and 0.17 respectively for the pion, muon-damped and neutron sources. The corresponding values of R_{exp} are given as $0.90, 0.45,$ and 2.16 respectively. Scenario TBM corresponds to the case where the true value of θ_{23} is maximal, while Scenario 2 exemplifies a situation where the true value of θ_{23} is non-maximal and $> \pi/4$. We checked that the results for $\theta_{23} < \pi/4$ share the same features as the ones for $\theta_{23} > \pi/4$.

We show the results of our χ^2 fit using T only in Fig. 3. The left panels show results for Scenario TBM while the right panels are for Scenario 2. The upper, middle and lower panels are for pion, muon-damped and neutron sources, respectively. In each panel the current 1σ and 3σ limits on $\sin^2 \theta_{23}$ are given. We have allowed for impure sources by choosing initial flux compositions of $(1 : 2 : 0), (0 : 1 : 0)$ and $(1 : 0 : 0), (1 : 1.9 : 0), (0.05 : 1 : 0)$ and $(1 : 0.05 : 0),$ as well as $(1 : 1.8 : 0), (0.1 : 1 : 0)$ and $(1 : 0.1 : 0)$ for pion, muon-damped and neutron sources, respectively. Interestingly, impurity affects the neutron sources more strongly, and the impact is slightly larger on the “dark-side” of $\sin^2 \theta_{23}$, i.e., for $\theta_{23} \geq \pi/4$. The “mexican hat” shape for pion and muon-damped sources is easy to understand by looking at the $\sin^2 \theta_{23}$ dependence of T in Fig. 2. Therefore, for pion and muon-damped sources we get, in general, a two-fold degeneracy for every value of T . For Scenario 2 we get slightly larger values for T and are hence no longer at the bottom of the parabolic shape. Therefore, the χ^2 minima lie at lower and larger values of $\sin^2 \theta_{23}$ and the two possible values of $\sin^2 \theta_{23}$ become further separated.

From Fig. 3 we can infer that considering only the pion or muon-damped flavor ratio will bring limited information on $\sin^2 \theta_{23}$. Indeed for these two sources and for Scenario TBM, we get an allowed 1σ range that is much bigger than the current 1σ range. With neutron sources, we get an allowed 1σ range for $\sin^2 \theta_{23}$ from 0.42 to 0.64 , which is a bit smaller than the current 3σ range. For Scenario 2 (true value $\sin^2 \theta_{23} > 1/2$) we would not be able to corroborate it with either the pion or muon-damped sources, in particular because we obtain two allowed regions for $\sin^2 \theta_{23}$. With neutron sources, and their linear dependence on $\sin^2 \theta_{23}$, we expect to get only one allowed zone. The plot confirms this and in addition we see that in this case maximal mixing is ruled out by neutrino telescope data alone. To be more precise, from measuring T with neutron sources we could constrain $\sin^2 \theta_{23}$ to be greater than 0.54 at the 1σ level and greater than 0.5 at 90% C.L.

Since these conclusions depend on the errors considered for the flavor ratios, we have generalized our analysis and studied the allowed range of $\sin^2 \theta_{23}$ as a function of the error. In Fig. 4 we display the results. The upper 4 panels are for data generated for the TBM case while the lower 2 are for the neutron sources only and data corresponding to Scenario 2. For TBM in data and with pion and muon-damped sources, we can infer that even for an extremely small error of the order of 5%, the allowed range at 90% C.L. is bigger than the current ones. Neutron sources can impose an upper limit only for very small errors. A lower limit can be imposed if the error on the flavor ratio is smaller than 18%. If Scenario 2 was true, then neutron sources could rule out maximal mixing and give information on the octant of θ_{23} , and Fig. 4 shows that the T ratio is better suited than R for this purpose.

To improve the sensitivity of neutrino telescopes to θ_{23} , one should combine measure-

ments of T from different sources. In Fig. 5 we have considered the combination of pion and muon-damped sources (upper panels), of pion and neutron sources (middle panels) and of all the three different type of sources (lower panels). The χ^2 function is, for example,

$$\chi^2 = \left(\frac{(T_\pi)_{\text{th}} - (T_\pi)_{\text{exp}}}{\sigma_{(T_\pi)_{\text{exp}}}} \right)^2 + \left(\frac{(T_\mu)_{\text{th}} - (T_\mu)_{\text{exp}}}{\sigma_{(T_\mu)_{\text{exp}}}} \right)^2 + \sum_{ij=12,13} \left(\frac{s_{ij}^2 - (s_{ij}^2)_{\text{best-fit}}}{\sigma_{s_{ij}^2}} \right)^2 \quad (18)$$

when measurements from pion and muon-damped sources are combined. The left panels show results for the Scenario TBM, while the right panels showcase Scenario 2. It should be noted that the two-fold degeneracy with respect to $\sin^2 \theta_{23}$ is hardly present anymore when two or more T ratios are combined. Three different cases are plotted in the figures. With “pure” we refer to initial flavor compositions $(1 : 2 : 0)$, $(0 : 1 : 0)$ and $(1 : 0 : 0)$, with “impure A” we refer to $(1 : 1.9 : 0)$, $(0.05 : 1 : 0)$ and $(1 : 0.05 : 0)$, while for “impure B” we refer to $(1 : 1.8 : 0)$, $(0.1 : 1 : 0)$ and $(1 : 0.1 : 0)$. Again, the effect of impurity is stronger for $\sin^2 \theta_{23} > 1/2$. In general, impurity shifts the χ^2 minimum to larger values of $\sin^2 \theta_{23}$. Analyzing the plots, we can conclude that the combinations of pion and muon-damped sources will not give us precise information on $\sin^2 \theta_{23}$ and that only the combination with neutron sources improves substantially the sensitivity. Indeed, we can notice that the combined constraint from pion and neutron sources looks basically identical to the result of neutron sources alone (see Fig. 3). Moreover, if all three sources are combined, i.e., if muon-damped sources are added, hardly any improvement is seen. For Scenario 2, we could determine the octant of θ_{23} at the 1σ level in case we combine T_π and T_n or all the three flavor ratios. We can, therefore, conclude that the importance of the neutron source is crucial to provide a good sensitivity to $\sin^2 \theta_{23}$.

Better constraints on θ_{23} are obtained when the ratios T and R are combined. The χ^2 function is now the same as in Eq. (16) with an appropriate term including R added. The result of the minimization is shown in Fig. 6, and the improvement with respect to the other plots is obvious. The effect of impurity is however stronger. This is understandable from the approximate expressions of T and R in Eqs. (13, 15), in which the impurity factors ζ and η have more sizable prefactors in R .

To summarize, once one combines T and R , the χ^2 curves become less broad, but the shift due to impurity becomes more sizable. The best constraint is obtained by combining T and R for neutron sources. Indeed, Fig. 6 shows that the 1σ range for $\sin^2 \theta_{23}$ is of the same order as the current one. For Scenario 2 we can exclude maximal mixing at roughly 90% C.L. level. This conclusion depends also on the error considered for R . Varying it we show in Fig. 4 the allowed range of $\sin^2 \theta_{23}$ if only R was measured.

The most optimistic scenario would occur when both ratios can be measured for all three sources. We checked that the outcome is basically identical to combining T and R for neutron sources, showing once again that these sources are best suited for θ_{23} constraints.

We stress that throughout this study we have tried to extract information on only the mixing angle θ_{23} and assumed that the kind of astrophysical source is known. Note that the values for the T and R ratios of different sources are well separated even if the errors on the flux ratios are bigger than the ones we are considering. In addition, the neutron

beams, for which the sensitivity to $\sin^2 \theta_{23}$ is stronger, have the advantage that the ratio T is rather small, and R is very large. This will allow more easily to distinguish one source from the others. A detailed analysis on the problematics related to the determination of the type of source is beyond the task of this work and will be published separately.

4 Summary and Conclusions

Neutrino mixing affects the flux ratios of ultra high energy neutrinos arriving on earth. The exact values of the ratios are determined by the values of the mixing parameters. A series of papers have looked into the impact of standard and non-standard properties of neutrinos on the flux ratios. In this paper we argued that within the framework of the standard picture with three stable neutrinos, the mixing angle θ_{23} has the maximum effect on the flux ratios. We performed a statistical test to ascertain quantitatively the extent to which this mixing angle can be constrained by measuring the flux ratios of ultra high energy neutrinos.

We defined two kind of flux ratios, $T = \Phi_\mu/\Phi_{\text{tot}}$ and $R = \Phi_e/\Phi_\tau$, where $\Phi_{\text{tot}} = \Phi_e + \Phi_\mu + \Phi_\tau$. We showed the dependence of these ratios on the mixing angles θ_{13} and θ_{23} for three kinds of sources of ultra high energy neutrinos – pion, muon-damped and neutron sources. Their dependence on θ_{23} is largest, and from analytical considerations we gave an idea of the extent to which the flux ratios could be used to constrain it.

We defined a χ^2 function to quantify the extent to which θ_{23} can be constrained by neutrino telescopes. We assumed a simplistic approach where we worked with the flux ratios themselves but we are aware that in a realistic analysis one should work with ratios of actual number of events, taking into account the detector response and efficiencies. However, we have chosen to work in a simplified set-up because the purpose of this paper was to make a ballpark estimate of the sensitivity of neutrino telescopes to θ_{23} . For the first time we included “impure” initial neutrino fluxes in a statistical analysis by introducing two variables, ζ and η , which parameterize deviations from the initial flux compositions $(1 : 2 : 0)$, $(0 : 1 : 0)$ or $(1 : 0 : 0)$ for the pion, muon-damped and neutron sources.

We performed the statistical analysis using T from one given source at a time and conclude that the best θ_{23} sensitivity comes from neutron sources. We showed that an error of less than 20 % is necessary to obtain results comparable to oscillation experiments. We presented results by combining pion and neutron sources, muon-damped and neutron sources, and finally all three taken together. The bound improves mainly because neutron sources have a much better handle on θ_{23} . We next combined T and R measurements at the neutrino telescopes. Adding the information of R improves the θ_{23} bound substantially, but increases somewhat the impact of impure sources. In particular, we note that the combination of T and R for neutron sources could give us bounds on θ_{23} which are much better than the one we have currently. In fact, measuring T and R for neutron sources could be comparable to the bounds on θ_{23} we expect from future long baseline and atmospheric neutrino experiments, depending of course on the uncertainty on the measurement of the flux ratios at the neutrino telescopes. We performed the statistical test on θ_{23} for true

$\sin^2 \theta_{23} = 0.5$ and $\sin^2 \theta_{23} = 0.6$. For the latter case we checked if it would be possible to establish the right octant of θ_{23} .

In conclusion, in favorable but not unrealistic situations we can indeed expect useful and complementary limits on θ_{23} which are comparable to the ones from dedicated oscillation experiments.

Acknowledgments

We would like to thank J. Kopp and M. Lindner for helpful discussions. V.N. and W.R. were supported by the Deutsche Forschungsgemeinschaft in the Sonderforschungsbereich Transregio 27 “Neutrinos and beyond – Weakly interacting particles in Physics, Astrophysics and Cosmology”. S.C. acknowledges support from the Neutrino Project under the XI Plan of Harish-Chandra Research Institute.

References

- [1] J. Ahrens *et al.* [The IceCube Collaboration], Nucl. Phys. Proc. Suppl. **118**, 388 (2003) [astro-ph/0209556].
- [2] A. Achterberg *et al.* [IceCube Collaboration], Astropart. Phys. **26**, 155 (2006) [arXiv:astro-ph/0604450].
- [3] Information available at <http://www.km3net.org>
- [4] J. G. Learned and S. Pakvasa, Astropart. Phys. **3**, 267 (1995).
- [5] S. Pakvasa, Mod. Phys. Lett. A **19**, 1163 (2004) [Yad. Fiz. **67**, 1179 (2004)] [hep-ph/0405179].
- [6] M. L. Costantini and F. Vissani, Astropart. Phys. **23**, 477 (2005); F. Vissani, Astropart. Phys. **26**, 310 (2006); astro-ph/0609575.
- [7] P. Bhattacharjee and N. Gupta, hep-ph/0501191.
- [8] P. D. Serpico and M. Kachelriess, Phys. Rev. Lett. **94**, 211102 (2005).
- [9] P. D. Serpico, Phys. Rev. D **73**, 047301 (2006).
- [10] Z. Z. Xing and S. Zhou, Phys. Rev. D **74**, 013010 (2006).
- [11] W. Winter, Phys. Rev. D **74**, 033015 (2006).
- [12] Z. Z. Xing, Phys. Rev. D **74**, 013009 (2006).
- [13] M. Kachelriess and R. Tomas, Phys. Rev. D **74**, 063009 (2006).

- [14] D. Majumdar and A. Ghosal, Phys. Rev. D **75**, 113004 (2007).
- [15] W. Rodejohann, JCAP **0701**, 029 (2007).
- [16] D. Meloni and T. Ohlsson, Phys. Rev. D **75**, 125017 (2007).
- [17] R. L. Awasthi and S. Choubey, Phys. Rev. D **76**, 113002 (2007).
- [18] K. Blum, Y. Nir and E. Waxman, arXiv:0706.2070 [hep-ph].
- [19] M. Kachelriess, S. Ostapchenko and R. Tomas, Phys. Rev. D **77**, 023007 (2008).
- [20] G. R. Hwang and K. Siyeon, arXiv:0711.3122 [hep-ph].
- [21] S. Pakvasa, W. Rodejohann and T. J. Weiler, Phys. Rev. Lett. **100**, 111801 (2008) [arXiv:0711.0052 [hep-ph]]
- [22] S. Pakvasa, W. Rodejohann and T. J. Weiler, JHEP **0802**, 005 (2008).
- [23] B. T. Cleveland *et al.*, Astrophys. J. **496**, 505 (1998); J. N. Abdurashitov *et al.* [SAGE Collaboration], J. Exp. Theor. Phys. **95**, 181 (2002) [Zh. Eksp. Teor. Fiz. **122**, 211 (2002)]; W. Hampel *et al.* [GALLEX Collaboration], Phys. Lett. B **447**, 127 (1999); S. Fukuda *et al.* [Super-Kamiokande Collaboration], Phys. Lett. B **539**, 179 (2002); B. Aharmim *et al.* [SNO Collaboration], Phys. Rev. C **72**, 055502 (2005); C. Arpesella *et al.* [Borexino Collaboration], Phys. Lett. B **658**, 101 (2008).
- [24] Y. Ashie *et al.* [Super-Kamiokande Collaboration], Phys. Rev. D **71**, 112005 (2005).
- [25] T. Araki *et al.* [KamLAND Collaboration], Phys. Rev. Lett. **94**, 081801 (2005); S. Abe *et al.* [KamLAND Collaboration], arXiv:0801.4589 [hep-ex].
- [26] E. Aliu *et al.* [K2K Collaboration], Phys. Rev. Lett. **94**, 081802 (2005).
- [27] D. G. Michael *et al.*, [MINOS Collaboration], arXiv:hep-ex/0607088.
- [28] M. C. Gonzalez-Garcia and M. Maltoni, arXiv:0704.1800 [hep-ph]; M. Maltoni, T. Schwetz, M. A. Tortola and J. W. F. Valle, New J. Phys. **6**, 122 (2004), hep-ph/0405172v5; S. Choubey, arXiv:hep-ph/0509217; S. Goswami, Int. J. Mod. Phys. A **21**, 1901 (2006); A. Bandyopadhyay, S. Choubey, S. Goswami, S. T. Petcov and D. P. Roy, Phys. Lett. B **608**, 115 (2005); G. L. Fogli *et al.*, Prog. Part. Nucl. Phys. **57**, 742 (2006).
- [29] M. Apollonio *et al.*, Eur. Phys. J. C **27**, 331 (2003).
- [30] P. Lipari, M. Lusignoli and D. Meloni, Phys. Rev. D **75**, 123005 (2007).
- [31] M. C. Gonzalez-Garcia, M. Maltoni and A. Y. Smirnov, Phys. Rev. D **70**, 093005 (2004) and references therein.

- [32] S. Choubey and P. Roy, Phys. Rev. D **73**, 013006 (2006).
- [33] S. Choubey, arXiv:hep-ph/0609182 and references therein.
- [34] P. Huber, M. Lindner, M. Rolinec, T. Schwetz and W. Winter, Phys. Rev. D **70**, 073014 (2004) and references therein.
- [35] P. F. Harrison, D. H. Perkins and W. G. Scott, Phys. Lett. B **530**, 167 (2002); Phys. Lett. B **535**, 163 (2002); Z. Z. Xing, Phys. Lett. B **533**, 85 (2002); X. G. He and A. Zee, Phys. Lett. B **560**, 87 (2003); see also L. Wolfenstein, Phys. Rev. D **18**, 958 (1978); Y. Yamanaka, H. Sugawara and S. Pakvasa, Phys. Rev. D **25**, 1895 (1982) [Erratum-ibid. D **29**, 2135 (1984)].
- [36] J. P. Rachen and P. Meszaros, Phys. Rev. D **58**, 123005 (1998); T. Kashti and E. Waxman, Phys. Rev. Lett. **95**, 181101 (2005).
- [37] L. A. Anchordoqui, H. Goldberg, F. Halzen and T. J. Weiler, Phys. Lett. B **593**, 42 (2004).
- [38] J. F. Beacom, N. F. Bell, D. Hooper, S. Pakvasa and T. J. Weiler, Phys. Rev. D **68**, 093005 (2003) [Erratum-ibid. D **72**, 019901 (2005)].
- [39] L. Anchordoqui and F. Halzen, Annals Phys. **321**, 2660 (2006).
- [40] F. Ardellier *et al.*, arXiv:hep-ex/0405032.

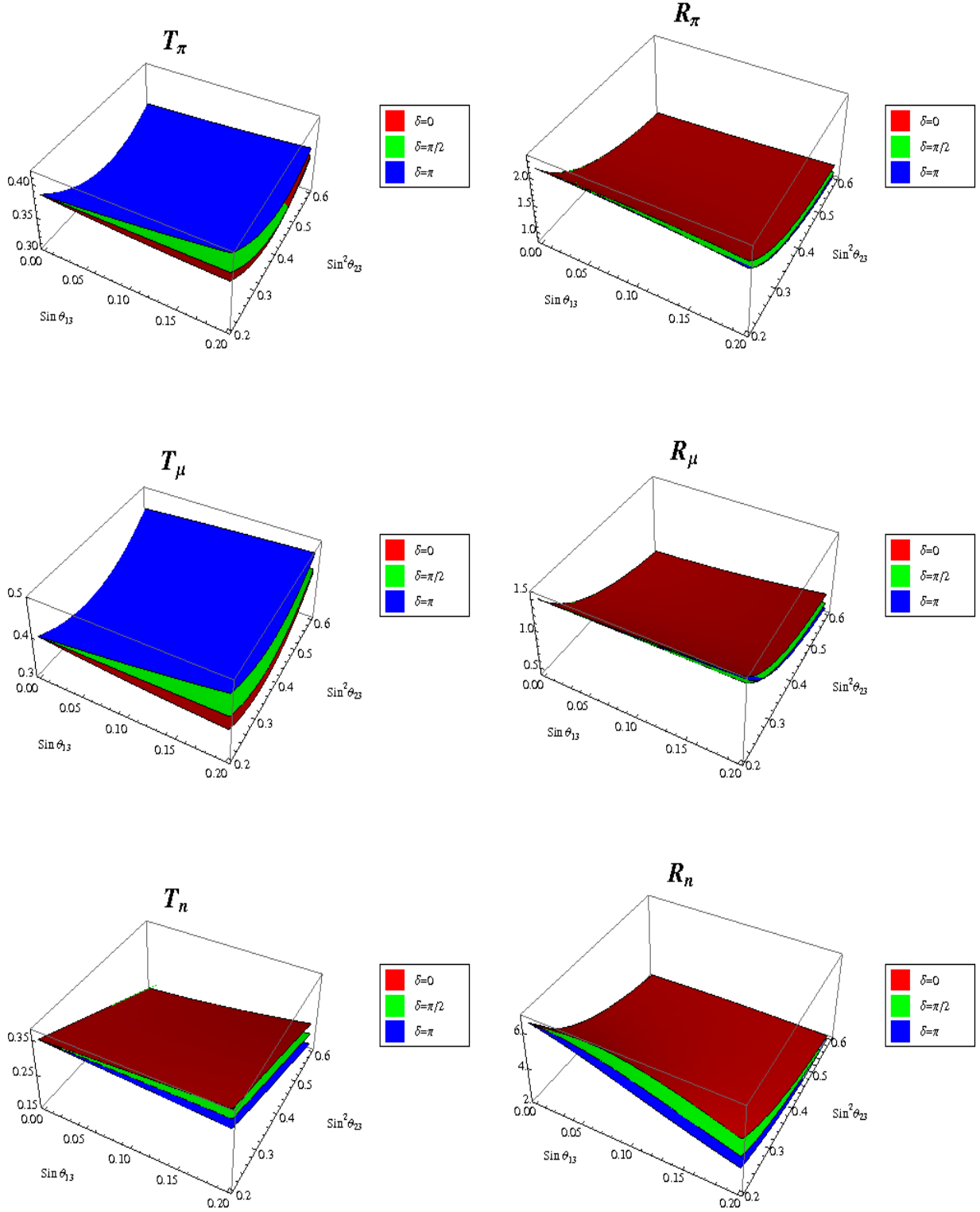


Figure 1: The ratios $T = \Phi_\mu/\Phi_{\text{tot}}$ (left panel) and $R = \Phi_e/\Phi_\tau$ (right panel) for the three sources under discussion as a function of $\sin \theta_{13}$ and $\sin^2 \theta_{23}$. The mixing angle θ_{12} has been fixed to its best-fit value, i.e., $\sin^2 \theta_{12} = 0.32$.

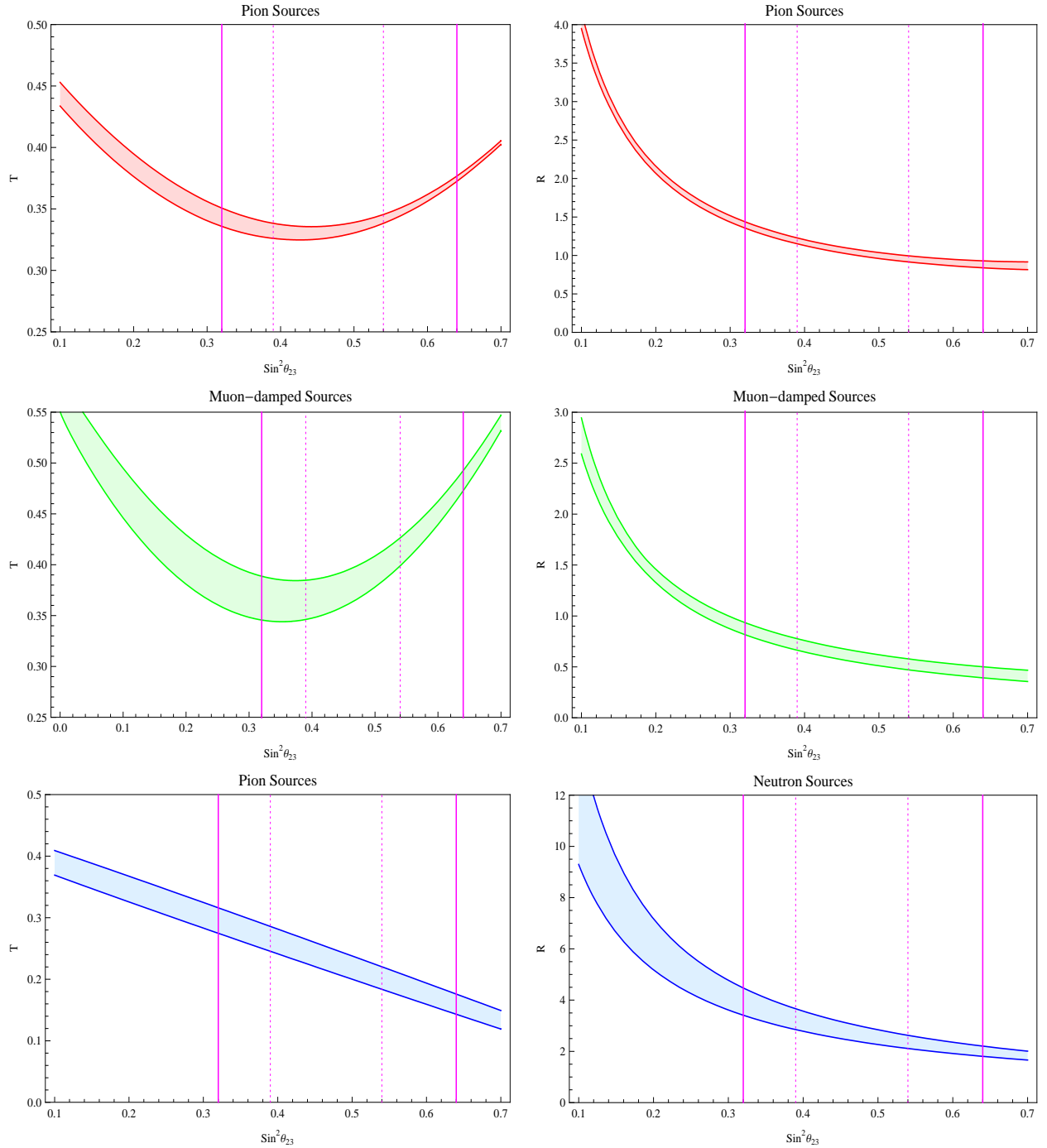


Figure 2: The ratios $T = \Phi_\mu / \Phi_{\text{tot}}$ (left panel) and $R = \Phi_e / \Phi_\tau$ (right panel) for the three sources as a function of $\sin^2 \theta_{23}$ when the ranges of the mixing parameters are $\sin^2 \theta_{12} = 0.32 \pm 0.02$ and $\sin^2 \theta_{13} \leq 0.005$. The current 1σ and 3σ ranges of $\sin^2 \theta_{23}$ are also indicated.

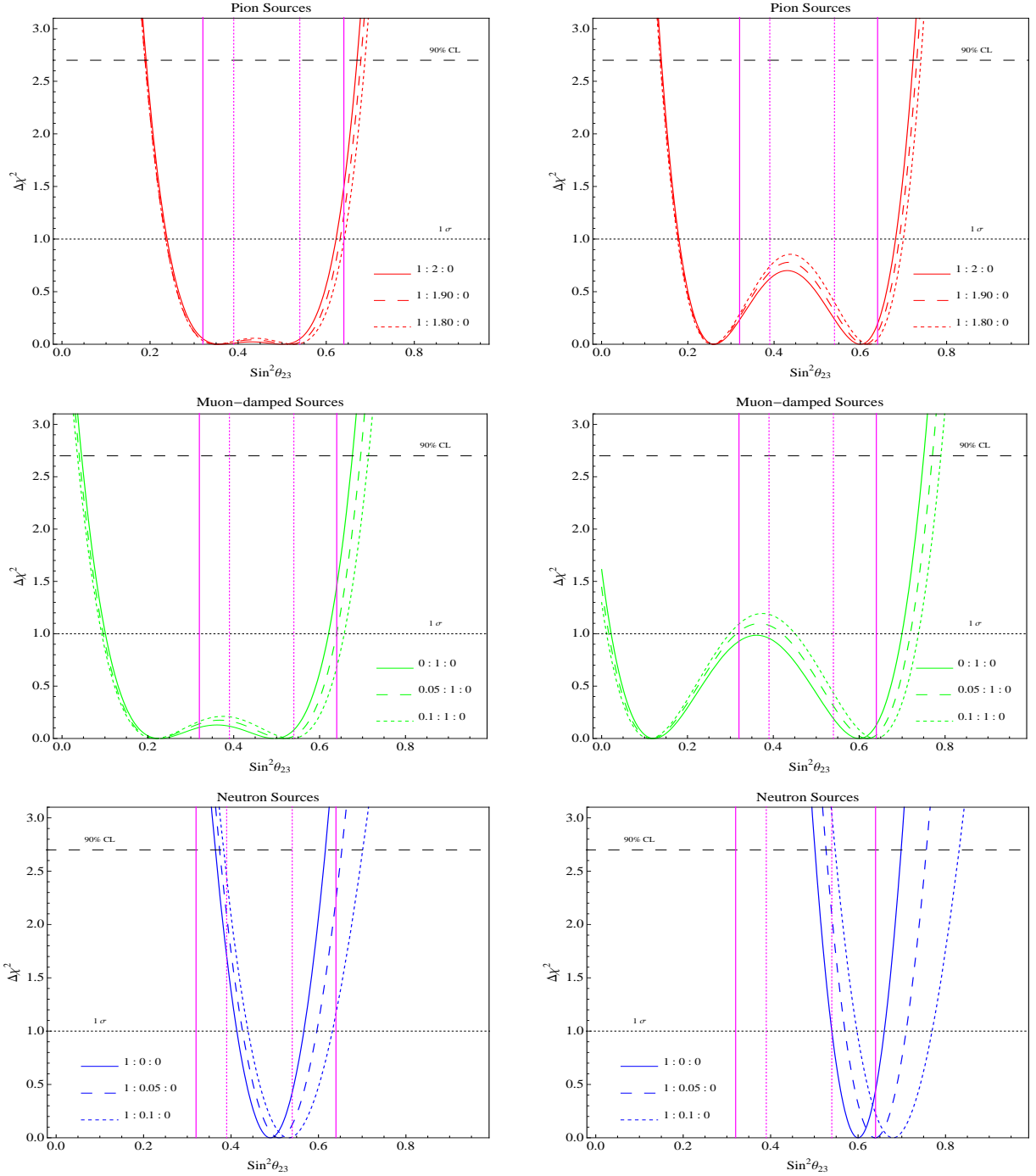


Figure 3: Constraints on $\sin^2 \theta_{23}$ from a χ^2 analysis obtained by measuring the ratio $T = \Phi_\mu / \Phi_{\text{tot}}$ for the three different neutrino sources. The left panel assumes the “tribimaximal values” $T = \frac{1}{3}$, $\frac{7}{18}$ and $\frac{2}{9}$ as experimental values, while the right panel is for “true values” of the mixing angles given by Scenario 2. The current 1σ and 3σ ranges of $\sin^2 \theta_{23}$ are also indicated.

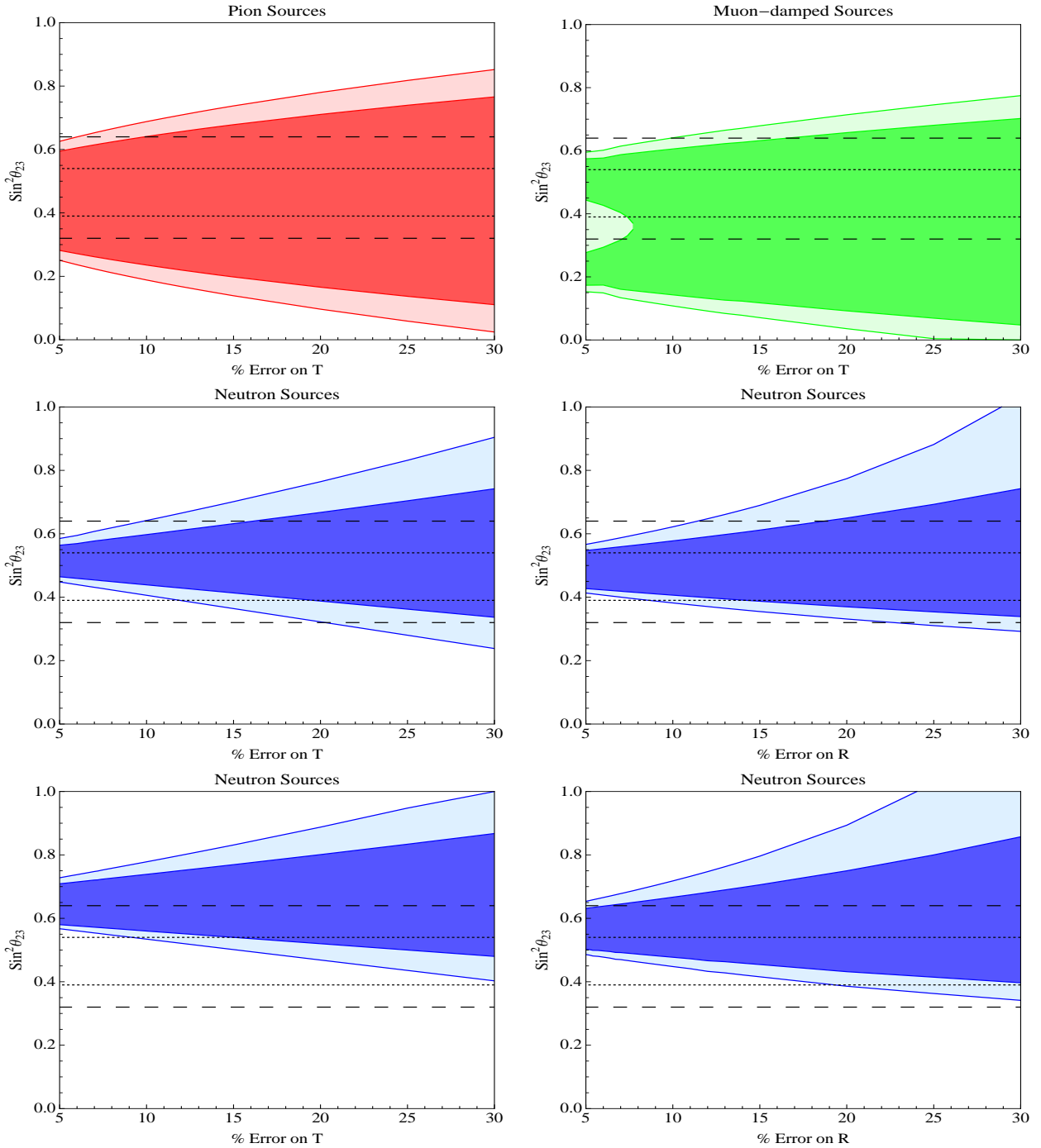


Figure 4: Allowed range of $\sin^2 \theta_{23}$ as a function of the error on the flavor ratio. The dark areas represent the 1σ range, while the lighter areas are at 90% C.L. The upper 4 plots are for scenario TBM, the 2 lower ones for scenario 2, where we only plot neutron sources. The current 1σ and 3σ ranges of $\sin^2 \theta_{23}$ are also indicated.

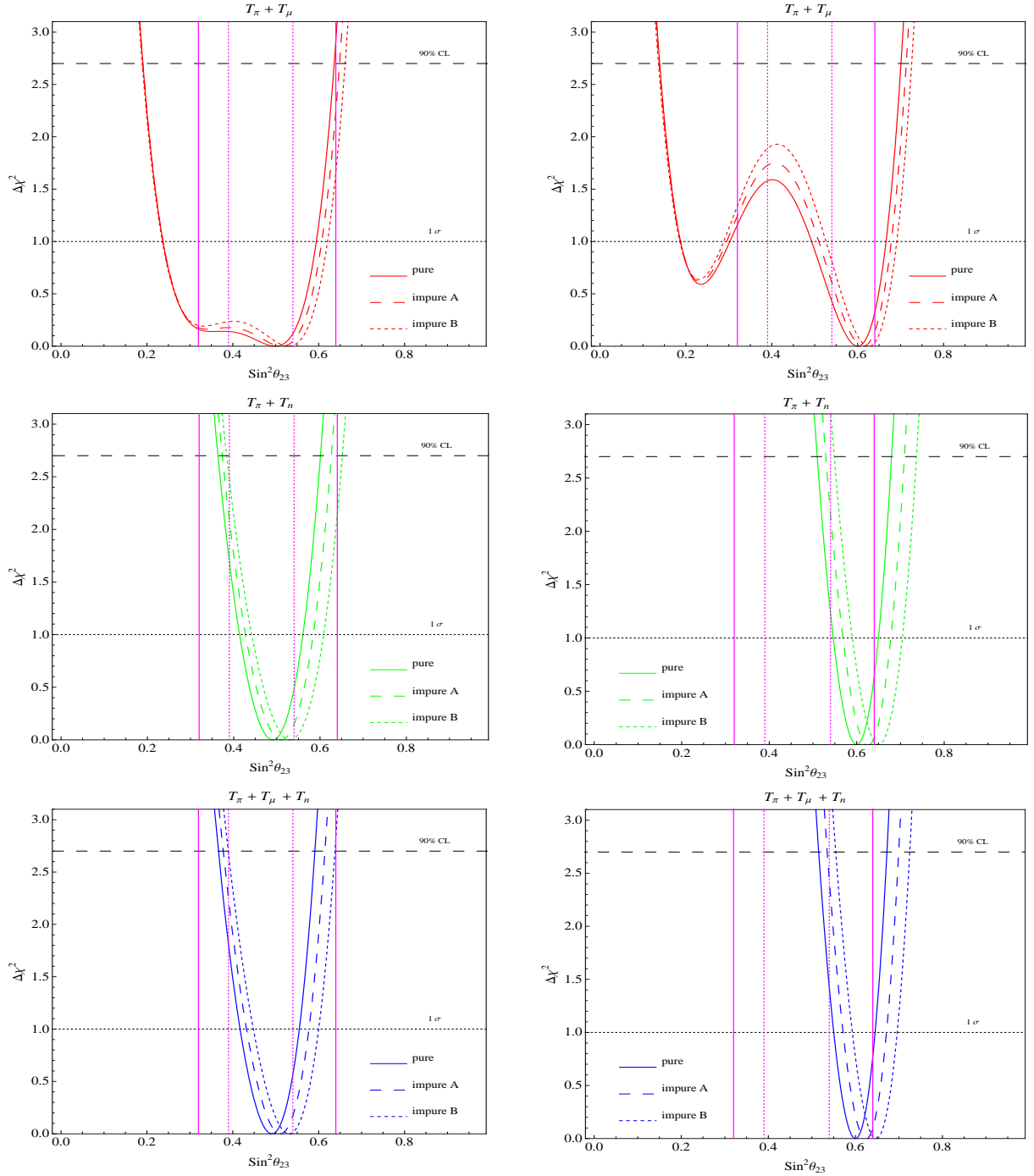


Figure 5: Same as Fig. 3, but for combined measurements of T from different sources. With “pure” we refer to the initial flavor composition $(1 : 2 : 0)$, $(0 : 1 : 0)$ and $(1 : 0 : 0)$, with “impure A” we refer to $(1 : 1.9 : 0)$, $(0.05 : 1 : 0)$ and $(1 : 0.05 : 0)$, while for “impure B” we refer to $(1 : 1.8 : 0)$, $(0.1 : 1 : 0)$ and $(1 : 0.1 : 0)$.

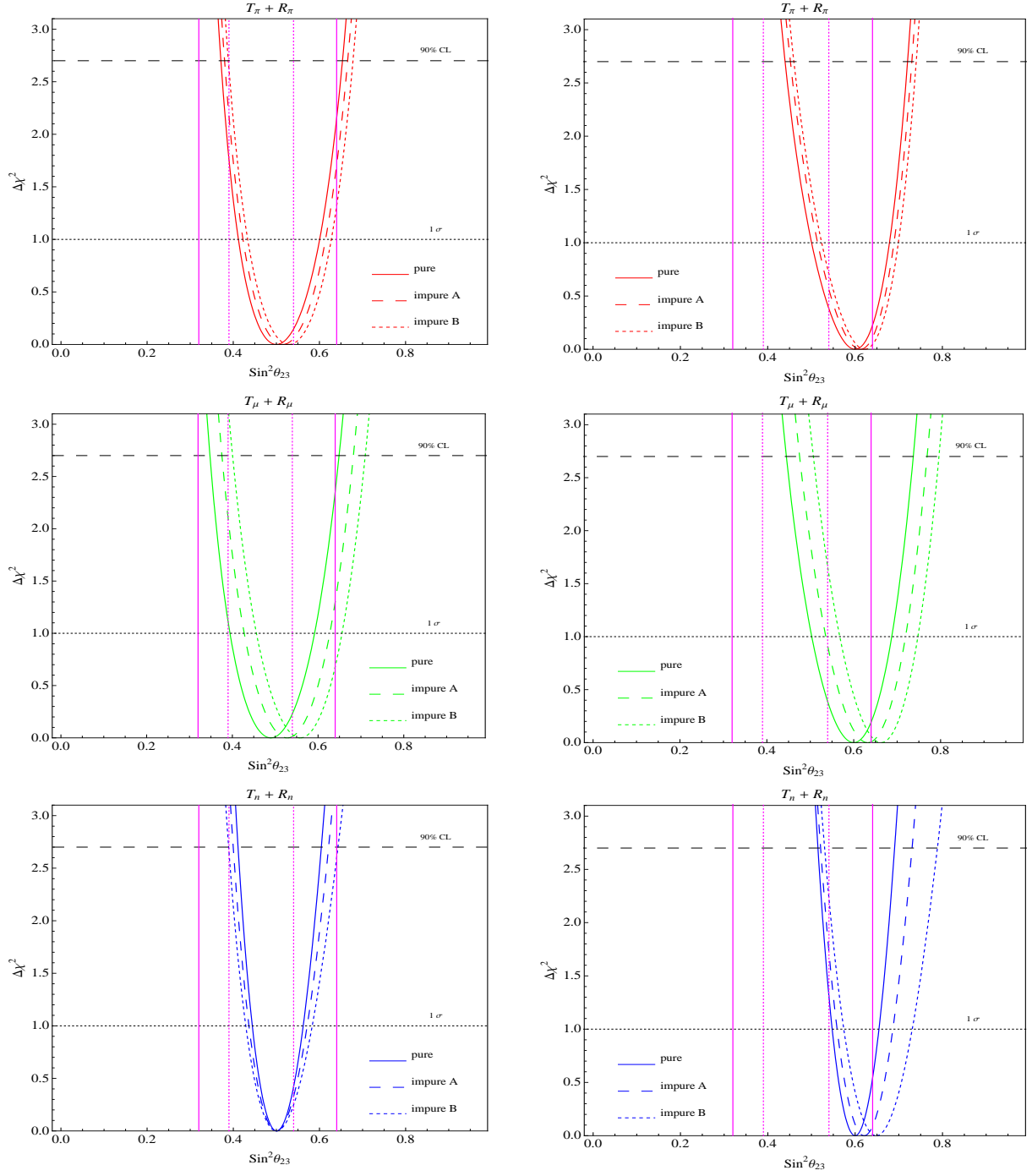


Figure 6: Same as Fig. 3, but for combined measurements of T and R ratios.